HHS Public Access

Author manuscript

Transl Res. Author manuscript; available in PMC 2025 January 01.

Published in final edited form as:

Transl Res. 2024 January ; 263: 15–27. doi:10.1016/j.trsl.2023.08.002.

Transcription factor EBF1 mitigates neuropathic pain by rescuing Kv1.2 expression in primary sensory neurons

Yingping Liang[1,*], **Dilip Sharma**[1,*], **Bing Wang**[1,*], **Huixing Wang**[1,*], **Xiaozhou Feng**[1], **Ruining Ma**[1], **Tolga Berkman**[1], **Steven Char**[1], **Alex Bekker**[1], **Yuan-Xiang Tao**[1,2,3,†]

[1]Department of Anesthesiology, New Jersey Medical School, Rutgers, The State University of New Jersey, Newark, NJ 07103, USA

[2]Department of Physiology, Pharmacology & Neuroscience, New Jersey Medical School, Rutgers, The State University of New Jersey, Newark, NJ 07103, USA

[3]Departments of Cell Biology & Molecular Medicine, New Jersey Medical School, Rutgers, The State University of New Jersey, Newark, NJ 07103, USA.

Abstract

Nerve injury-induced alternations of gene expression in primary sensory neurons of dorsal root ganglion (DRG) are molecular basis of neuropathic pain genesis. Transcription factors regulate gene expression. In this study, we examined whether early B cell factor 1 (EBF1), a transcription factor, in the DRG participated in neuropathic pain caused by chronic constriction injury (CCI) of the sciatic nerve. EBF1 was distributed exclusively in neuronal nucleus and co-expressed with cytoplasmic/membrane Kv1.2 in individual DRG neurons. The expression of *Ebf1* mRNA and protein was time-dependently downregulated in the ipsilateral lumbar (L) 3/4 DRGs after unilateral CCI. Rescuing this downregulation through microinjection of the adeno-associated virus 5 expressing full-length *Ebf1* mRNA into the ipsilateral L3/4 DRGs reversed the CCI-induced decrease of DRG Kv1.2 expression and alleviated the development and maintenance of mechanical, heat and cold hypersensitivities. Conversely, mimicking the downregulation of DRG EBF1 through microinjection of AAV5-expressing *Ebf1* shRNA into unilateral L3/4 DRGs produced a reduction of Kv1.2 expression in the ipsilateral L3/4 DRGs, spontaneous pain and the enhanced responses to mechanical, heat and cold stimuli in naive mice. Mechanistically, EBF1 not only bound to *Kcna2* gene (encoding Kv1.2) promoter but also directly activated its

[†]**Corresponding author:** Dr. Yuan-Xiang Tao, Department of Anesthesiology, New Jersey Medical School, Rutgers, The State University of New Jersey, 185 S. Orange Ave., MSB, F-661, Newark, NJ 07103. Tel: +1-973-972-9812; Fax: +1-973-972-1644. yuanxiang.tao@njms.rutgers.edu.

[*]These authors contributed equally to this work.

AUTHOR CONTRIBUTIONS

Y.X.T. conceived the project and supervised most experiments. Y.L., D.S., B.W., H.W., X.F., R.M., T.B. and Y.X.T. designed the project. Y.L. and D.S. performed the animal model, conducted behavioral experiments, and carried out microinjection. X.F. constructed the vectors and carried out ChiP and luciferase assays. Y.L., D.S., B.W. and H.W. performed Western blot and real-time RT-PCR assays. R.M. and T.B. were involved in parts of animal model conductance, behavioral testing, or microinjection. Y.L., X.F. and Y.X.T. analyzed the data. Y.L and Y.X.T. wrote the draft of manuscript. S.C., A.B. and Y.X.T. edited and finalized the manuscript. All authors have read the journal's authorship agreement, reviewed and approved the manuscript for publication.

activity. CCI decreased the EBF1 binding to *Kcna2* promoter in the ipsilateral L3/4 DRGs. Our findings suggest that DRG EBF1 downregulation contributes to neuropathic pain likely by losing its binding to *Kcna2* promoter and subsequently silencing Kv1.2 expression in primary sensory neurons. Exogenous EBF1 administration may mitigate neuropathic pain by rescuing DRG Kv1.2 expression.

Keywords

EBF1; Kv1.2; dorsal root ganglion; neuropathic pain

Background

Neuropathic pain resulting from damage caused by injury and/or diseases in peripheral or central nervous system affects 7%–10% of the world population.[1,2] The clinical manifestations of neuropathic pain presents as ongoing or intermittent spontaneous pain (e.g., burning, shooting, pricking, pins, needles, and freezing pain) and evoked pain (such as mechanical allodynia and heat hyperalgesia), often accompanied by neuropathic pain-associated anxiety or depression.[1,2] Current available medications such as opiates and nonsteroidal anti-inflammatory drugs are often ineffective and/or have severe side effects (e.g., hyperalgesia, tolerance or addiction).[3,4] As such, it is imperative to develop new drugs. Peripheral nerve injury leads to abnormal transcription of pain-related genes in primary sensory neurons of the dorsal root ganglion (DRG), resulting in changes in their expression at the protein level such as Kv1.2 downregulation.[5–14] These changes contribute to the development and maintenance of neuropathic pain.[10,15,16] Understanding how these pain-related genes are altered in the DRG after peripheral nerve injury may provide a new avenue for the management of this disorder.

The transcription factor Early B cell factor 1 (EBF1) is a member of the Collier/Olf1/EBF family of transcription factors, which are critical for development processes (including cell fate decisions), cell migration and cell differentiation.[17] EBF1 is essential for expressing key proteins required for B cell differentiation, as the mice with EBF1 knockout exhibited a complete block at the pre-pro-B-cell stage.[18] Conversely, overexpression of EBF1 in hematopoietic stem cells or multilineage progenitors produced the increased formation of B lymphocytes at the expense of other lineages, indicating the instructive capacity of EBF1.[19] Moreover, EBF1 also regulates the differentiation of adipocytes[20] and sensory neurons.[20–22] Increasing evidence suggests that EBF1 plays a crucial role in metabolic and inflammatory signaling pathways in mature adipocytes.[23] However, whether EBF1 in sensory neurons of adult DRG participates in nerve injury-induced changes of pain-associated genes and has a functional role in neuropathic pain is still unknown.

In this study, we first examined the expression and distribution of EBF1 in the DRG and whether its expression was altered following chronic constriction injury (CCI) of unilateral sciatic nerve or unilateral fourth lumbar spinal nerve ligation (SNL) in mice. We then determined whether this alternation was required and sufficient for the development and

maintenance of CCI-induced nociceptive hypersensitivity. Finally, we elucidated how this alternation contributed to CCI-induced neuropathic pain.

Materials and methods

Animal preparations

CD1 male and female mice (about 7–8 weeks, weighed 20–25g) were purchased from Charles River Laboratories (Wilmington, MA). Mice were maintained in the animal facility at 23 ± 2 °C under an automatic 12 h light/dark cycle and provided with food and water as desired. To minimize inter-individual variability in behavioral outcome measurements, mice were acclimatized for at least two days before behavioral experiments. The experimenters were blinded to group assignment and treatment conditions. The current study was performed in compliance with the ethics guidelines laid down in the Declaration of Helsinki. All procedures used were approved by the Animal Care and Use Committee of Rutgers New Jersey Medical School, following the ethical guidelines of the National Institutes of Health and the International Association for the Study of Pain.

Neuropathic pain models

The preclinical mouse model of CCI-induced neuropathic pain was carried out as previously described.[24–26] Briefly, after the mice were anesthetized with 2–3% isoflurane, the unilateral sciatic nerve was exposed and loosely ligated with 7–0 silk thread at three sites with an interval of about 1 mm proximal to the trifurcation of the sciatic nerve. Sham mice were subjected to the same surgery but without ligation.

The preclinical mouse model of SNL-induced neuropathic pain was also performed as stated previously.[14,27–29] In brief, after the experimental mice were anesthetized as stated above, the unilateral fourth lumbar (L4) transverse process was identified and removed. The underlying L4 spinal nerve was isolated carefully, ligated with a 7–0 silk suture and then transected just distal to the ligature. Sham mice received an identical surgery but without transection and ligation of the L4 spinal nerve.

DRG microinjection

DRG microinjection was carried out according to the procedure used in our previous studies.[14,27–29] Briefly, after the mice were anesthetized as described above, the unilateral L3/4 articular processes were removed and the corresponding L3/4 DRGs were exposed. AAV5 (1 μl/DRG, 4–5×10^{12} GC/mL) was microinjected into the exposed DRGs for 10 minutes through a glass micropipette connected to a Hamilton syringe under dissection microscopy. After microinjection, the pipette was retained for 10 minutes before it was removed. Finally, the surgical field was irrigated with sterile saline and closed with wound clips.

Behavioral tests

The evoked pain tests including mechanical, heat and cold tests were performed in order with 1-hour intervals as reported previously.[14,27–29] The conditional place preference (CCP)

test was carried out as described previously[14,27–29] on week 8 after microinjection. The locomotor test was completed as stated previously[14,27–29] before tissue collection.

For the mechanical test, two calibrated von Frey filaments (0.07 and 0.4 g, Stoelting Co.) were used to measure paw withdrawal frequencies in response to mechanical stimuli. Briefly, the mouse was placed individually in a Plexiglas chamber on an elevated mesh screen. Each von Frey filament was applied to the plantar side of both hind paws. Each trial was repeated 10 times at 5 min intervals. A quick paw withdrawal was identified as a positive response. Paw withdrawal frequency was calculated by the number of positive responses within 10 trials.

For the heat test, the Model 336 Analgesic Meter (IITC Life Science Inc.) was employed to evaluate paw withdrawal latencies to heat stimulation. In brief, the mice were placed in individual Plexiglas chambers on a glass plate. The middle plantar surface of each hind paw was exposed to a beam of light from the lightbox. The light beam was automatically turned off once the hind paw was quickly lifted. The length of time between the start and stop of the light beam was recorded as the paw withdrawal latency. Three trials were performed with 5 min-intervals between each trial. An automatic cut-off time of 20 seconds was used to avoid hind paw tissue damage.

For the cold test, mice were placed in an individual Plexiglas chamber on the cold aluminum plate (−1~0°C) to assess paw withdrawal latency to cold stimulation. The temperature of the aluminum plate was monitored continuously by a thermometer. The duration time between the placement of mice on the aluminum plate and the sign of mouse jumping was recorded as the paw withdrawal latency. Each trial was repeated for 3 times at 30-mins intervals. A cut-off time of 20 s was used to avoid tissue damage.

For the CPP test, an apparatus with two individual Plexiglas chambers connected with an internal door (Med Associates Inc., Vermont, US) was used. One chamber is composed of a rough floor and four walls with black and white horizontal stripes and another is made of a smooth floor and four walls with black and white vertical stripes. The time spent on each chamber was monitored by photobeam detectors installed along the chamber walls and automatically recorded in MED-PC IV CPP software. All mice were preconditioned for 30 minutes to habituate the environment with free access to two chambers. The base residence time was then recorded in each chamber within 15 minutes. The mice that spent more than 80% or less than 20% of the total time in each chamber were excluded from further testing. The conditional test was carried out for the following 3 days as the internal door was closed. The mice first received an intrathecal injection of saline (5 μl) specifically paired with one conditioning chamber for 30 minutes in the morning. Six hours later, lidocaine (0.8 % in 5 μl saline) was intrathecally injected and paired with another conditioning chamber for 30 minutes. The sequence of saline and lidocaine administration was switched each day. On the fourth day, mice were placed in the chamber with the internal door open and freely able to access to each chamber. Within 15-minutes, the time each mouse stayed in the chamber was recorded. Difference scores were calculated by subtracting preconditioning time from test time spent in the lidocaine chamber.

For locomotor testing, placing, grasping and righting reflexes were performed. (1) Placing reflex: the positions of the hind limbs were placed slightly lower than those of the forelimbs and the dorsal surfaces of the hind paws were brought into contact with the edge of a table. Whether the hind paws were placed on the table surface reflexively was recorded. (2) Grasping reflex: after the mice were placed on a wire grid, whether the hind paws grasped the wire on contact was recorded. (3) Righting reflex: once the mice were placed back on a flat surface, whether they immediately assumed normal upright position was recorded. Each trial was repeated 5 times at 5-minutes intervals. The scores for each reflex were recorded based on counts of each normal reflex.

Cell culture and transfection

DRG neuronal cultures were prepared according to previously described methods.[30,31] Briefly, after the 4-week CD1 mice were euthanized with an overdose of isoflurane, all DRGs were harvested into a cold Neurobasal medium (Gibco/Thermo Fisher Scientific) with 10% fetal bovine serum (Gibco/Thermo Fisher Scientific), 2% B-27 Supplement (Gibco/Thermo Fisher Scientific), 1% L-Glutamine (Gibco/Thermo Fisher Scientific), 100 units/ml penicillin and 100 μg/ml streptomycin (Gibco/Thermo Fisher Scientific). The DRGs were then treated with enzyme solution (5 mg/ml dispase and 1 mg/ml collagenase type I in Hanks'balanced salt solution without Ca^{2+} and Mg^{2+} (Gibco/Thermo Fisher Scientific)) at 37°C for 20 minutes. After trituration and centrifugation, the dissociated cells were resuspended in a mixed neurobasal medium and filtrated with a 70-μm cell strainer. The DRG neurons were plated onto poly-D-lysine (Sigma, USA)-coated six-well plates at the density of $1\times10^6/cm^2$ cells and cultured at 37°C in a 5% CO_2 atmosphere. On the second day, the AAV5 virus (10~15 μl/well, titer $\geqslant1\times10^{12}$) was added to each well based. The cultured neurons were harvested for Western blot analysis described below 3 days later.

Western blotting assay

Protein extraction and Western immunoblotting were carried out according to published protocols.[14,27–29] Briefly, DRGs or spinal cord were homogenized and the cultured cells ultrasonicated on ice with the lysis buffer (10 mM Tris, 1 mM phenylmethylsulfonyl fluoride, 5 mM $MgCl_2$, 5 mM EGTA, 1 mM EDTA, 1mM DTT, 40 μM leupeptin, 250 mM sucrose). The pellet (nuclear fraction) and the supernatant (membrane/cytosolic fractions) were separated and collected, respectively, after centrifugation at 1,000 g for 15 minutes at 4°C. The pellet was then treated with the lysis buffer containing 2% sodium dodecyl sulfate and 0.1% Triton X-100. The amounts of proteins in the samples were measured using the Bio-Rad protein assay (Bio-Rad). Twenty μg per sample were loaded onto a 4–15% stacking/7.5% separating SDS-polyacrylamide gel (12-well; Bio-Rad Laboratories, Hercules, CA). The protein was then electrophoretically transferred onto a polyvinylidene difluoride membrane (Bio-Rad Laboratories). After the membrane was first incubated in the blocking buffer (5% nonfat milk plus 0.1% Tween-20 in the Tris-buffered saline) for 1 hour at room temperature, they were incubated with primary antibodies at 4°C overnight. The primary antibodies included rabbit anti-EBF1 (1:1,000, Invitrogen), rabbit anti-histone H3 (1:1,000, Santa Cruz), rabbit anti-ERK1/2 (1:1,000, Cell Signaling Technology), rabbit anti-phosphorylated ERK1/2 (p-ERK1/2; 1:1,000, Cell Signaling Technology), mouse anti-GFAP (1:1,000, Cell Signaling Technology), rabbit anti-GAPDH (1:3,000, Santa Cruz)

and mouse anti-Kv1.2 (1:1,000, R&D systems). The proteins were detected by horseradish peroxidase–conjugated anti-rabbit and anti-mouse secondary antibodies (1:5,000, Jackson ImmunoResearch) at room temperature for 1 hour and visualized by western peroxide reagent and luminol/enhancer reagent (Clarity Western ECL Substrate, Bio-Rad) using ChemiDoc XRS System with Image Lab software (Bio-Rad). The intensity of the band was quantified with densitometry using Image J software. The relative density values from different time points after CCI or sham surgery were calculated by dividing the densities from these time points by the density at the corresponding 0 day after each was normalized to its corresponding H3 (for nuclear protein) or GAPDH (for cytoplasmic/membrane proteins) density. The relative density value at 0 day was calculated by dividing each repeat density by average density among 3 biological repeats after each repeat was normalized to its corresponding H3 or GAPDH density.

Quantitative real-time RT-PCR

RNA extraction and quantitative real-time RT-PCR assay were carried out according to our published protocol.[14,27–29] Briefly, Total RNA was extracted from the DRG by using TRIzol-chloroform methods (Invitrogen), treated with an overdose of deoxyribonuclease I (New England Biolabs), and reverse-transcribed with the ThermoScript Reverse Transcriptase (Invitrogen/Thermo Fisher Scientific) and oligo(dT) primers (Invitrogen/Thermo Fisher Scientific). The template (4 μl) was amplified in a Bio-Rad CFX96 real-time PCR system by using the following primers for *Ebf1* mRNA or *Tuba1a* mRNA (Supplementary Table 1). Each sample was repeated 3 times with a 20-μl reaction volume containing 200 nM forward and reverse primers, 10 μl of SsoAdvanced Universal SYBR Green Supermix (Bio-Rad Laboratories), and 20 ng of cDNA. The PCR amplification included 30 seconds at 95°C, 30 seconds at 60°C, 30 seconds at 72°C, and 5 minutes at 72°C for 39 cycles. All PCR data were normalized to an internal control *Tuba1a*. The ratios of mRNA levels at the different time points post-surgery to mRNA levels at day 0 were calculated using the ΔCt method ($2^{-\Delta\Delta Ct}$).

Immunofluorescent histochemistry

Double-labeled immunofluorescent histochemistry was carried out as described previously.[6–8] In brief, after being anesthetized with an overdose of isoflurane, mice were perfused with 50 ml of 0.01 M phosphate-buffered saline (PBS; pH 7.4) followed by 100 ml of 4% paraformaldehyde in 0.01 M PBS. Bilateral L3/4 DRGs were collected, post-fixed in the same fixative solution at 4°C for 2 hours and cryoprotected in 30% sucrose in 0.01 M PBS overnight. DRGs were cut at the thickness of 15 μm on a cryostat. All sections were pretreated with acetone for 15 minutes and then blocked with 0.01 M PBS containing 5% goat serum and 0.3% Triton X-100 at 37°C for 1 hour. The sections were incubated with rabbit anti-EBF1 (1:400, Millipore Sigma), mouse anti-neurofilament 200 (NF200; 1:200, Millipore Sigma), mouse anti-Kv1.2(1:300, Neuromab), biotinylated IB4 (IB4; 1:100, Sigma), and mouse anti-CGRP (1:50, Abcam), mouse anti-glutamine synthetase (GS; 1:400, Sigma), mouse anti-tyrosine hydroxylase(TH; 1:1,000, Thermo Fisher) and chicken anti-β tubulin III (1:1,000, Abcam) at 4°C overnight. On the second day, after being washed for 5 minutes three times in 0.01 M PBS, the sections were incubated with goat anti-rabbit antibody conjugated with Cy3 (1:200, Jackson ImmunoResearch), goat anti-mouse antibody

or anti-chicken antibody conjugated with Cy2 (1:200, Jackson ImmunoResearch), or avidin labeled with FITC (1:200, Sigma) for 1 hour at room temperature. Control experiments were carried out in parallel as previously reported. Under a Leica DMI4000 fluorescence microscope (Leica) with a DFC365 FX camera (Leica), the immunofluorescent images were captured.

Plasmid construction and virus production

To construct a plasmid expressing EBF1 or Kv1.2 protein, the full-length sequence of *Ebf1* mRNA or *Kcan2* mRNA from the mouse's DRG was reverse-transcribed using the SuperScript IV One-Step RT qPCR System with Platinum Taq High Fidelity DNA Polymerase (ThermoFisher Scientific) and amplified by PCR with specific primers (Supplementary Table 1). The PCR product was inserted into the corresponding sites of the pHpa-tra-SK plasmids (University of North Carolina, Chapel Hill) to replace the enhanced GFP sequence. The resulting vectors expressed the *Ebf1* mRNA under the control of the cytomegalovirus promoter. The *Ebf1* shRNA duplex was designed according to bases 13–36 of the mouse *Ebf1* mRNA (GenBank accession number NM_ 001290709). The oligonucleotides harboring the shRNA sequences were synthesized and annealed. A control shRNA with a scrambled sequence and no homology to a mouse gene was used as a control. The fragments were ligated into the pro-viral plasmid (pAAV5-U6-shRNA) by BamH1/XbaI restriction sites. AAV5 packaging was performed by using the AAVpro purification kit (Takara, Mountain View, CA). The virus titer was assessed by using the AAVpro Titration Kit (Takara).

Luciferase Assay

The 1,816- bp fragment from the *Kcan2* gene promotor region (including the EBF1- binding motif) was amplified by PCR from genomic DNA with the primers (Supplementary Table 1) in order to construct the *Kcna2* gene reporter plasmid. The PCR products were ligated into the *KpnI* and *XhoI* restriction sites of the pGL3- Basic vector (Promega, Madison, WI). The sequences of recombinant clones were verified by DNA sequencing. The CAD cells were plated on a 12- well plate and cultured at 37 °C in a humidified incubator with 5% CO_2. One day after culture, the cells of each well were co- transfected with 300 ng of plasmids, 300 ng of pGL3- Basic vector with or without the sequences of *Kcan2* promoter, and 10 ng of the pRL-TK (Promega) by using Lipofectamine 3000 (Invitrogen), according to the manufacturer's instructions. Two days after transfection, the cells were collected and lysed in a passive lysis buffer. Approximately 10 μl of supernatant was used to measure the luciferase activity using the Dual- Luciferase Reporter Assay System (Promega). Independent transfection experiments were repeated three times. The relative reporter activity was calculated after normalization of the firefly activity to the renilla activity.

Chromatin immunoprecipitation (ChIP) Assay

The ChIP assays were carried out by using the EZ ChIP Kit (Upstate/EMD Millipore) as described previously.[5,8,32] The homogenate from the DRG was crosslinked with 1% formaldehyde at room temperature for 10 minutes. The reaction was stopped by the addition of glycine (0.25 M). After centrifugation, the pellet was collected and lysed in the SDS

lysis buffer containing the protease inhibitor cocktail. The lysis was sonicated until the DNA was sheared into fragments with a mean length of 200 to 1000 nt. The samples were first pre-cleaned with protein G magnetic beads and then subjected to immunoprecipitation overnight with 2.5 μg of rabbit anti-EBF1 antibody or with 2.5 μg of normal rabbit serum overnight at 4 °C. The input (10% of the sample for immunoprecipitation) was used as a positive control. After purification, the DNA fragments were amplified using PCR/Real-time PCR with the primers listed in supplementary Table 1.

Statistical analysis

The cells and mice were randomly divided into different groups. The results presented as means ± SEM were assumed to be normal distribution based on previous studies.[4;30] The data were analyzed with a two-tailed, unpaired Student t-test or one-way or two-way ANOVA by using GraphPad Prism 8. When ANOVA showed significant differences, the post hoc Tukey test was used to compare the difference between two groups. Statistical significance was set at $P < 0.05$.

Results

Cellular distribution of EBF1 in dorsal root ganglion

To determine the role of DRG EBF1 in neuropathic pain, we first examined its cellular distribution in the DRG. Double labeling of EBF1 with β-tubulin III (a specific neuronal marker) or glutamine synthetase (GS, a marker for satellite glial cells) was carried out. Nuclear EBF1 co-expressed with cytoplasmic β-tubulin III in some individual cells (Fig. 1A), but was not expressed in the GS-labeled cells, from naive mice (Fig. 1B), indicating EBF1 is distributed exclusively in DRG neurons. About 39% (1,397 in 3,579) of β-tubulin III labeled neurons were positive for EBF1. Cross-sectional area analysis of neuronal somata showed that approximately 31.4% of EBF1-labelled neurons were small (< 500 μm^2 in the area), 39.2% were medium (500–1000 μm^2 in the area), and 29.4% were large (> 1,000 μm^2 in the area) (Fig. 1C). Consistently, about 32% of EBF1-labelled neurons were positive for NF200 (a marker for medium/large neurons and myelinated Ab fibers; Fig. 1D), 34% for CGRP (a marker for small DRG peptidergic neurons; Fig. 1E), 31% for IB4 (a marker for small nonpeptidergic neurons; Fig. 1F) and 20% for tyrosine hydroxylase (TH, a marker for small low-threshold neurons; Fig. 1G). The characterization of EBF1 distribution in DRG neurons suggests its involvement in transmission and modulation of nociceptive information.

Downregulation of EBF1 expression in injured dorsal root ganglion after peripheral nerve injury

We then asked if EBF1 expression was altered in the DRG after peripheral nerve injury. Consistent with previous studies,[24–26] mechanical allodynia demonstrated by significant increases in paw withdrawal frequencies in response to 0.07 g and 0.4 g von Frey filament stimuli and heat and cold hyperalgesia evidenced by marked decreases in paw withdrawal latencies in response to heat and cold stimuli, respectively, were seen on days 3, 7 and 14 after CCI on the ipsilateral, not contralateral, side (Fig. 2A–2D). Sham surgery did not alter basal paw withdrawal responses on either side (Fig. 2A–2D). Paralleling with these behavioral changes, in a time-dependent manner, EBF1 was downregulated in the ipsilateral

L3/4 DRGs, but not contralateral L3/4 DRGs and ipsilateral L3/4 spinal cord dorsal horn, after CCI (Fig. 2E). The level of EBF1 protein was decreased by 45%, 84% and 60% on days 3, 7 and 14 after CCI, respectively, as compared with the corresponding sham mice (Fig. 2E). Consistently, the amounts of *Ebf1* mRNA in the ipsilateral L3/4 DRGs on days 3, 7, and 14 after CCI were significantly less than those after sham surgery at the corresponding time points (Fig. 2F). Similar results were seen in injured DRG after SNL (Fig. 2G and 2H). The levels of EBF1 protein and *Ebf1* mRNA were decreased by 56% and 56%, respectively, in the ipsilateral L4 DRG on day 7 after SNL, as compared to those after sham surgery (Fig. 2G and 2H). Furthermore, the number of EBF1–positive neurons in the ipsilateral L3/4 DRGs on day 7 after CCI was decreased by 51.1% compared with the corresponding sham group (Fig. 2 I). However, CCI did not alter the distribution of EBF1-positive neuronal somata in injured DRG, as about 31.2% of EBF1-positive neurons were small, 39.2% were medium and 29.6% were large in the ipsilateral L3/4 DRGs on day 7 after CCI (Fig. 2J).

Rescuing downregulated DRG EBF1 mitigates the development of neuropathic pain

Does downregulated EBF1 in injured DRG participate in CCI-induced nociceptive hypersensitivity? To answer this question, we examined the effect of rescuing DRG EBF1 expression through microinjection of AAV5 expressing full-length *Ebf1* mRNA (AAV5-*Ebf1*) into the ipsilateral L3/4 DRGs 28 days before surgery on the development of CCI-induced nociceptive hypersensitivity in male mice, as AAV5 takes 3–4 weeks to become expressed.[24–26] AAV5 expressing GFP (AAV5-*Gfp*) was used as a control. As expected, the levels of EBF1 protein and its mRNA in the ipsilateral L3/4 DRGs from the AAV5-*Gfp*-microinjected CCI mice were dramatically reduced by 56% and 56%, respectively, of the values from the AAV5-*Gfp*-microinjected sham mice on day 14 post-surgery (Fig. 3A and 3B). These reductions were not found in the AAV5-*Ebf1*-microinjected CCI mice (Fig. 3A and 3B). The amounts of EBF1 protein and its mRNA in the ipsilateral L3/4 DRGs from the AAV5-*Ebf1*-microinjected sham mice were significantly increased by 1.67-fold and 1.74-fold, respectively, as compared to the AAV5-*Gfp*-microinjected sham mice on day 14 after surgery (Fig. 3A and 3B).

We further examined the behavioral responses of CCI or sham male mice after AAV5 microinjection. Like the observation above, mechanical allodynia and heat and cold hyperalgesia were seen on the ipsilateral side from days 3 to 14 after CCI in the AAV5-*Gfp*-microinjected mice (Fig. 3C–3F). DRG microinjection of AAV5-*Ebf1* significantly alleviated the CCI-induced increases in paw withdrawal frequencies in response to 0.07 g and 0.4 g von Frey filament stimuli (Fig. 3C and 3D) as well as the CCI-induced reductions in paw withdrawal latencies to heat (Fig. 3E) and cold (Fig. 3F) stimuli from days 3 to 14 post-CCI. DRG microinjection of neither AAV5 altered basal responses on the contralateral side of CCI mice and on either side of sham mice during the observation period (Fig. 3C–3I) and locomotor activity (Supplementary Table 2). In addition, DRG microinjection of AAV5-*Ebf1* mitigated the evoked stimulation-independent spontaneous ongoing pain demonstrated by a decrease in preference for the lidocaine-paired chamber on day 14 post-CCI (Fig. 3J and 3K). Sham mice with DRG microinjection of either virus did not exhibit any marked preference for two chambers (Fig. 3J and 3K).

DRG neuronal hyperexcitability triggers the hyperactivation of spinal cord dorsal horn neurons and astrocytes through enhancing the release of neurotransmitters/neuromodulators in primary afferents under neuropathic pain conditions.[33] To further confirm our behavioral observations above, we also examined whether DRG microinjection of AAV5-*Ebf1* had an impact on the CCI-induced neuronal and astrocyte hyperactivations in the dorsal horn of male mice. Consistent with previous reports,[24–26] the levels of p-ERK1/2 (a marker for neuronal hyperactivation), but not total ERK1/2, and GFAP (a marker for astrocyte hyperactivation) were substantially elevated in the ipsilateral L3/4 dorsal horn on day 14 after CCI in the AAV5-*Gfp*-microinjected CCI mice (Fig. 3L). These elevations were not found in the AAV5-*Ebf1*-microinjected CCI mice (Fig. 3L). Neither AAV5 changed basal levels of total ERK1/2, p-ERK1/2 or GFAP in the ipsilateral L3/4 dorsal horn of sham mice (Fig. 3L).

The results were similar in female CCI or sham mice after DRG viral microinjection (Fig. 4A–4L).

Overall, these results indicate that DRG overexpression of EBF1 may attenuate the development of CCI-induced nociceptive hypersensitivity and dorsal horn central sensitization.

Rescuing downregulated DRG EBF1 attenuates the maintenance of neuropathic pain

We also examined the effect of DRG microinjection of AAV5-*Ebf1* on the maintenance of CCI-induced nociceptive hypersensitivity. We microinjected AAV5 14 days prior to CCI in male mice. On day 7 post-CCI, mechanical allodynia and heat and cold hyperalgesia developed on the ipsilateral side in both AAV5-*Gfp*- and AAV5-*Ebf1*-microinjected mice (Fig. 5A–5D). However, these nociceptive hypersensitivities were attenuated on days 14, 21 and 28 after CCI in the AAV5-*Ebf1*-microinjected mice (Fig. 5A–5D). Basal responses on the contralateral side did not change in either AAV5-*Ebf1*- or AAV5-*Gfp*-microinjected CCI mice (Fig. 5A–5C). On day 28 post-CCI, stimulation-independent spontaneous ongoing pain evidenced by marked preference for the lidocaine-paired chamber in the AAV5-*Gfp*-microinjected mice was significantly alleviated in the AAV5-*Ebf1*-microinjected mice (Fig. 5E and 5F). As anticipated, the amounts of EBF1 protein and its mRNA in the ipsilateral L3/4 DRGs decreased by 58% and 57%, respectively, from the values in the contralateral L3/4 DRGs on days 28 post-CCI in the AAV5-*Gfp*-microinjected mice (Fig. 5G and 5H). Of note, these decreases were not seen in the ipsilateral side of the AAV5-*Ebf1*-microinjected mice (Fig. 5G and 5H). Additionally, the elevations in the levels of p-ERK1/2 (not total ERK1/2) and GFAP in the ipsilateral L3/4 dorsal horn 28 days after CCI from the AAV5-*Gfp*-microinjected mice were not found in the AAV5-*Ebf1*-microinjected mice (Fig. 5I). Collectively, our findings demonstrate that DRG overexpression of EBF1 may also mitigate the maintenance of CCI-induced nociceptive hypersensitivity and dorsal horn central sensitization.

Mimicking nerve injury-induced DRG EBF1 downregulation leads to neuropathic pain–like symptoms in naive mice

To determine whether the downregulated DRG EBF1 was sufficient for nerve injury-induced nociceptive hypersensitivity, we examined the effect of DRG knockdown of EBF1 through microinjection of AAV5 expressing *Ebf1* shRNA (AAV5-*Ebf1* shRNA) into unilateral L3/4DRGs of naive male mice on nociceptive thresholds. AAV5 expressing scrambled shRNA (AAV5-Scr shRNA) was used as a control. As expected, the levels of EBF1 proteins and its mRNA in the ipsilateral L3/4 DRGs of the AAV5-*Ebf1* shRNA-microinjected mice were reduced by 52% and 54%, respectively, in comparison to the AAV5-Scr shRNA-microinjected mice 9 weeks post-microinjection (Fig. 6A and 6B). DRG microinjection of AAV5-Scr shRNA, but not AAV5-Scr shRNA, led to significant increases in paw withdrawal frequencies in response to 0.07 g and 0.4 g von Frey filament stimuli and decreases in paw withdrawal latencies in response to heat and cold stimuli from week 5 to at least week 9 after microinjection on the ipsilateral side (Fig. 6C–6F). Neither AAV5 changed basal responses on the contralateral side (Fig. 6C–6E) and locomotor function (Supplementary Table 2). In addition to evoked nociceptive hypersensitivity, DRG microinjection of AAV5-Scr shRNA led to evoked stimulation-independent nociceptive hypersensitivity demonstrated by robust preference for the lidocaine-paired chamber on week 8 post-microinjection (Fig. 6G and 6H). In contrast, DRG microinjection of AAV5-Scr shRNA did not show any preference for either saline-paired or lidocaine-paired chamber, indicating no nociceptive hypersensitivity (Fig. 6G and 6H). In addition, DRG microinjection of AAV5-*Ebf1* shRNA, but not AAV5-Scr shRNA, elevated the levels of p-ERK1/2 (but not total ERK1/2) and GFAP in the ipsilateral L3/4 dorsal horn 9 weeks after microinjection (Fig. 6I). Similar results were observed in naive female mice with DRG microinjection of AAV5-*Ebf1* shRNA or AAV5-Scr shRNA (Fig. 7A–7I). Taken together, our findings indicate that, in the absence of nerve injury, DRG downregulation of EBF1 can lead to both spontaneous and evoked nociceptive hypersensitivity.

Downregulated EBF1 participates in nerve injury-induced Kv1.2 decrease in injured DRG

Lastly, we investigated how the downregulated EBF1 in injured DRG contributed to nerve injury-induced nociceptive hypersensitivity. We used the online Jaspar software (https://jaspar.genereg.net/) and identified a consensus EBF1 binding motif at the distal promoter region (−1,351/−1,341) of *Kcna2* gene. Given that the reductions of *Kcna2* mRNA and its encoding Kv1.2 protein in injured DRG are required for neuropathic pain genesis,[6,8,12,13,34] we proposed that *Kcan2* gene might be a downstream target of EBF1 in injured DRG and mediated its function in nerve injury-induced nociceptive hypersensitivity. Consistent with previous studies,[6,8,12,13,29,35] the levels of *Kcna2* mRNA and Kv1.2 were decreased in the ipsilateral L3/4 DRGs on days 14 (Fig. 8A and Supplementary Fig. 1A) and 28 (Fig. 8B and supplementary Fig. 1B) post-CCI in the AAV5-*Gfp*-microinjected male mice. These decreases were completely rescued in the AAV5-*Ebf1*-microinjected male mice (Fig. 8A and 8B; Supplementary Fig. 1A and 1B). These effects of AAV5-*Ebf1* are specific, because DRG microinjection of AAV5-*Ebf1* did not alter the CCI-induced increases in the amounts of *Elf1* mRNA and ELF1 protein (Supplementary Fig. 1C and 1D) and decreases in the levels of *K2p1.1* mRNA and K2p1.1 protein (Supplementary Fig. 1E and 1F) in the ipsilateral L3/4 DRGs on day 14 post-CCI. As expected, DRG microinjection of AAV5-*Ebf1*

increased basal expression of EBF1 in the ipsilateral L3/4 DRGs of sham mice (Fig. 8A). Conversely, DRG microinjection of AAV5-*Ebf1* shRNA reduced the levels of *Kcna2* mRNA and Kv1.2 protein, without changing basal expression of *Elf1* mRNA, *K2p1.1* mRNA and their respective proteins in the ipsilateral L3/4 DRGs of naive male mice on week 9 after microinjection (Fig. 8C and Supplementary Fig. 2A–2E). Similar findings were seen in the female mice after DRG microinjection of AAV5-*Ebf1*/AAV5-*Gfp* or AAV5-*Ebf1* shRNA/AAV5-Scr shRNA (Supplementary Fig. 3A–3D). In *in vitro* DRG neuronal culture, co-transduction of AAV5-*Ebf1* shRNA plus AAV5-*Gfp1* reduced the levels of not only *Ebf1* mRNA and EBF1 protein but also *Kcna2* mRNA and Kv1.2 protein (Fig. 8D–8F). These reductions were completely reversed in the cultured DRG neurons co-transduced with AAV5-*Ebf1* shRNA plus AAV5-*Ebf1* (Fig. 8D–8F). As anticipated, co-transduction of AAV5-Scr shRNA plus AAV5-*Ebf1* in DRG cultured neurons significantly increased the amounts of *Ebf1* mRNA, *Kcan2* mRNA and their respective proteins (Fig. 8D–8F).

Furthermore, the luciferase assay revealed that co-transfection of full-length *Ebf1* vector, *Scrambled* shRNA vector plus *Kcna2* reporter vector significantly elevated the activity of the *Kcan2* promoter in *in vitro* CAD cells (Fig. 8G). This elevation was dramatically blocked in the CAD cells co-transfected with full-length *Ebf1* vector, *Ebf1* shRNA vector plus *Kcna2* reporter vector (Fig. 8G). The ChIP assay revealed that the fragment of the *Kcan2* promoter including the *Ebf1* binding motif could be amplified from the complex immunoprecipitated with EBF1 antibody in the nuclear fraction from the ipsilateral L3/4 DRGs on day 7 post-sham surgery (Fig. 8H). CCI decreased the binding of EBF1 to the *Kcna2* promoter, as evidenced by a 74% decrease in binding activity in the ipsilateral L3/4 DRGs on day 7 post-CCI, as compared to that post-sham surgery (Fig. 8H). Double-labeled immunofluorescent staining showed that about 52% of EBF1-labeled neurons are positive for Kv1.2 in the DRG (Fig. 8I).

Finally, we examined whether rescuing DRG Kv1.2 expression through microinjection of AAV5 expressing mouse full-length *Kcna2* mRNA (AAV5-Kv1.2) into the ipsilateral L3/4 DRGs impacted on the EBF1 downregulation-caused nociceptive hypersensitivity in naïve male mice. DRG co-microinjection of AAV5-Kv1.2, but not AAV5-*Gfp*, markedly mitigated the AAV5-*Ebf1* shRNA-induced elevations in paw withdrawal frequencies in response to 0.07 g and 0.4 g von Frey filament stimuli (Fig. 9A and 9B) and the AAV5-*Ebf1* shRNA-induced decreases in paw withdrawal latencies to heat (Fig. 9C) and cold (Fig. 9D) stimuli on weeks 5 and 7 post-AAV5 microinjection on the ipsilateral side. As expected, DRG microinjection of neither combined AAV5 affected basal responses on the contralateral side of AAV5-*Ebf1* shRNA-microinjected mice and either side of AAV5-Scr shRNA-microinjected mice (Fig. 9A–G). DRG co-microinjection of AAV5-Kv1.2 also significantly blocked the AAV5-*Ebf1* shRNA-evoked stimulation-independent nociceptive hypersensitivity (Fig. 9H and 9I) and the AAV5-*Ebf1* shRNA-evoked increases of the levels of p-ERK1/2 and GFAP) in the ipsilateral l3/4 dorsal horn (Fig. 9J) on week 7 post-microinjection. As predicted, the amounts of EBF1 in the AAV5-*Ebf1* shRNA plus AAV5-GFP group or plus AAV5-Kv1.2 group decreases by 52% and 54%, respectively, from the value of the AAV5-Scr shRNA plus AAV5-GFP group 7 weeks after microinjection (Fig. 9K). The level of Kv1.2 in the AAV5-*Ebf1* shRNA plus AAV5-GFP group was reduced by 50% from the value of the AAV5-Scr shRNA plus AAV5-GFP group 7 weeks

post-microinjection (Fig. 9L). This reduction was completely reversed in the AAV5-*Ebf1* shRNA plus AAV5-Kv1.2 group (Fig. 9L). Basal level of Kv1.2 in the AAV5-Scr shRNA plus AAV5-Kv1.2 group was increased by 2.04-fold as compared to that in the AAV5-Scr shRNA plus AAV5-GFP group 7 weeks post-microinjection (Fig. 9L).

Together, our findings suggest that Kv1.2 is a downstream target of EBF1 and mediates the role of EBF1 in injured DRG neurons under neuropathic pain conditions.

4. Discussion

Although intensive studies on neuropathic pain have been done for several decades, the mechanisms underlying this disorder are still incompletely understood. In the present study, we reported that EBF1 was expressed exclusively in DRG neurons and that peripheral nerve injury downregulated its expression in injured DRG. Rescuing this downregulation mitigated nerve injury-induced nociceptive hypersensitivity during the development and maintenance periods. DRG knockdown of EBF1 produced neuropathic pain-like symptoms in the absence of nerve injury. Mechanistically, downregulated EBF1 resulted in a reduction of its binding to *Kcnc2* promoter, subsequent silence of *Kcna2* mRNA transcription and a decrease of Kv1.2 protein expression in injured DRG. Our findings suggest that overexpressing EBF1 may relieve neuropathic pain through rescuing *Kcna2* mRNA expression in injured DRG neurons.

In contrast to the transcription factors ELF1,[26] OCT1,[25] C/EBPβ[36] and MZF1,[37] EBF1 was downregulated in injured DRG after peripheral nerve injury. Under normal conditions, EBF1 is highly expressed in the neuronal nuclei (but not in satellite cells) and distributed in all three types (small, medium, and large) of DRG neurons. CCI or SNL led to significant and time-dependent decreases of *Ebf1* mRNA and EBF1 protein expression in injured DRG. These decreases occur in all three types of DRG neurons, since the distribution pattern of EBF1-positive neurons in DRG was not changed after CCI. Given that these decreases were correlated with the development and maintenance of nerve injury-induced nociceptive hypersensitivity, our findings suggest that the downregulated EBF1 in injured DRG may be implicated in neuropathic pain. Our findings also revealed that DRG *Ebf1* gene was transcriptionally silenced following peripheral nerve injury. Although the detailed mechanisms of how nerve injury causes its transcriptional inactivation remains unclear, it may involve other downregulated transcription factors, or be caused by epigenetic silence or decreased RNA stability. These possibilities are to be explored in future studies.

Downregulated EBF1 results in a decrease of *Kcna2* mRNA and Kv1.2 protein expression in injured DRG under neuropathic pain conditions. Kv1.2 is one of the alpha subunits in the voltage-gated potassium (Kv) channels, which are critical for establishing resting membrane potential and controlling the excitability of DRG neurons.[13,34,38] Kv1.2 is highly expressed in DRG and distributed predominantly in medium and large DRG neurons.[34] Peripheral nerve injury reduced the expression of *Kcna2 mRNA* and Kv1.2 protein in the injured DRG.[39–42] Mimicking this reduction diminished total Kv current, depolarized the resting membrane potential, reduced current threshold for activation of action potentials and increased the number of action potentials in the DRG neurons, and leads to neuropathic pain

symptoms.[6,12,13,34,37] Rescuing this reduction attenuated the development and maintenance of nerve injury-induced nociceptive hypersensitivity.[6,12,13,34,37] DRG reduced Kv1.2 is likely one key factor that causes neuropathic pain. In the present study, we demonstrated that downregulated EBF1 transcriptionally silenced the *Kcna2* gene in injured DRG after peripheral nerve injury. Given that EBF1 is expressed in small, medium, and large DRG neurons, the present study chose AAV5 as the delivery vehicle to rescue or knock down DRG EBF1 expression, because it can transduce all three types of DRG neurons.[13,43,44] Rescuing DRG downregulation of EBF1 through DRG microinjection of AAV5-*Ebf1* not only alleviated the CCI-induced nociceptive hypersensitivity but also blocked the CCI-induced reductions in DRG *Kcna2* mRNA and Kv1.2 protein from both male and female mice. DRG knockdown of EBF1 through DRG microinjection of AAV5-*Ebf1* shRNA diminished basal expression of DRG *Kcna2* mRNA and Kv1.2 protein and led to nociceptive hypersensitivity-like behaviors in both male and female mice. These observed effects may not be attributed to DRG microinjection-caused tissue/cell damages, because the microinjected animals showed no signs of paresis or other abnormalities[6,12,13,34,37]. The injected DRG, stained with cresyl-violet and antibodies against other markers, retained their structural integrity and displayed no significant changes in numbers of neurons and satellite cells.[6,12,13,34,37] The present study also showed that the binding of EBF1 to the *Kcna2* promoter was significantly reduced in injured DRG after CCI. *In vitro* experiment showed that EBF1 overexpression specifically triggered the activation of *Kcna2* promotor activity. Given that nuclear EBF1 co-expressed with cytoplasmic/membrane Kv1.2 in individual DRG neurons and that rescuing DRG Kv1.2 reduction mitigated the EBF1 downregulation-caused nociceptive hypersensitivity, the antinociceptive effect caused by rescuing the CCI-induced downregulation of DRG EBF1 likely results from the failure to transcriptional silence of *Kcna2* gene in injured DRG after CCI. Without Kv1.2 reduction, no changes would occur in Kv1.2-mediated current, total Kv current, resting membrane potential and current threshold for activation of action potentials in the injured DRG neurons. Furthermore, the release of primary afferent transmitters/modulators and subsequent central sensitization in the ipsilateral dorsal horn would not occur. Consistent with this conclusion, we showed that rescuing the CCI-induced downregulation of DRG EBF1 completely blocked the CCI-induced increases in markers for hyperactivation in dorsal horn neurons and astrocytes. The evidence suggests that DRG EBF1 overexpression mitigates nerve neuropathic pain likely through rescuing Kv1.2 expression in injured DRG. It should be worth noting that, besides downregulated EBF1, other mechanisms such as *Kcan2* antisense long noncoding RNA,[13] G9a,[6] eIF4G2,[29] and DNMT3a[12] also contribute to nerve injury-induced decrease of DRG Kv1.2. Moreover, in addition to Kv1.2, EBF1 may transcriptionally regulate the expression of other pain-associated genes (e.g., *Tlr5*[45] and *Raly*[8]) because their promoters contain the EBF1-binding motif. Whether these genes participate in the function of DRG downregulated EBF1 in neuropathic pain remains to be determined. Additionally, peripheral nerve injury produces dysregulation in the expression of thousands of genes (including other transcription factors, ion channels, receptors and etc)[11]. Participation of these dysregulated genes in neuropathic pain genesis could not be excluded.

Conclusion

In summary, we have demonstrated how the downregulated EBF1 causes a decrease of Kv1.2 expression in injured DRG after peripheral nerve injury. Given that rescuing the nerve injury-induced DRG EBF1 downregulation through DRG microinjection of AAV5-*Ebf1* mitigates nerve injury-induced nociceptive hypersensitivity without changing basal or acute pain and locomotor function, Exogenous EFB1 delivered by AAV can be used as a potential antinociceptive drug in neuropathic pain management, as AAV has been used as a delivered vehicle for COVID-19 vaccine. However, potential side effects produced by EBF1 should be taken into considerations, as it is widely expressed in body tissues.

Supplementary Material

Refer to Web version on PubMed Central for supplementary material.

ACKNOWLEDGMENTS

All authors have read the journal's policy on disclosure of potential conflicts of interest. The authors declare no competing conflicts of interest. This work was supported by grants from the National Institutes of Health, Bethesda, Maryland (R01NS111553, R01NS117484 and RFNS113881).

Availability of data materials

All data and materials generated in this work are available upon request.

Abbreviations

DRG	dorsal root ganglion
EBF1	early B cell factor 1
CCI	chronic constriction injury
SNL	spinal nerve ligation
CCP	conditional place preference
TH	tyrosine hydroxylase
GS	glutamine synthetase
NF200	neurofilament 200
ChIP	chromatin immunoprecipitation

References:

1. Gaskin DJ, Richard P. The economic costs of pain in the United States. J. Pain 2012; 13: 715–724 [PubMed: 22607834]
2. Gilron I, Baron R, Jensen T. Neuropathic pain: principles of diagnosis and treatment. Mayo Clin. Proc 2015; 90: 532–545 [PubMed: 25841257]

3. Meyer R, Patel AM, Rattana SK, Quock TP, Mody SH. Prescription opioid abuse: a literature review of the clinical and economic burden in the United States. Popul. Health Manag 2014; 17: 372–387 [PubMed: 25075734]
4. Vorobeychik Y, Gordin V, Mao J, Chen L. Combination therapy for neuropathic pain: a review of current evidence. CNS. Drugs 2011; 25: 1023–1034 [PubMed: 22133325]
5. Du S, Wu S, Feng X, et al. A nerve injury-specific long noncoding RNA promotes neuropathic pain by increasing Ccl2 expression. J Clin Invest 2022; 132: e153563 [PubMed: 35775484]
6. Liang L, Gu X, Zhao JY, et al. G9a participates in nerve injury-induced Kcna2 downregulation in primary sensory neurons. Sci. Rep 2016; 6: 37704 [PubMed: 27874088]
7. Mo K, Wu S, Gu X, et al. MBD1 Contributes to the Genesis of Acute Pain and Neuropathic Pain by Epigenetic Silencing of Oprm1 and Kcna2 Genes in Primary Sensory Neurons. J. Neurosci 2018; 38: 9883–9899 [PubMed: 30266739]
8. Pan Z, Du S, Wang K, et al. Downregulation of a Dorsal Root Ganglion-Specifically Enriched Long Noncoding RNA is Required for Neuropathic Pain by Negatively Regulating RALY-Triggered Ehmt2 Expression. Adv. Sci. (Weinh.) 2021; 8: e2004515 [PubMed: 34383386]
9. Sun L, Gu X, Pan Z, et al. Contribution of DNMT1 to neuropathic pain genesis partially through epigenetically repressing Kcna2 in primary afferent neurons. J. Neurosci 2019
10. Wu S, Bono J, Tao YX. Long noncoding RNA (lncRNA): A target in neuropathic pain. Expert. Opin. Ther. Targets 2019; 23: 15–20 [PubMed: 30451044]
11. Wu S, Marie LB, Miao X, et al. Dorsal root ganglion transcriptome analysis following peripheral nerve injury in mice. Mol Pain 2016; 12: 1–14
12. Zhao JY, Liang L, Gu X, et al. DNA methyltransferase DNMT3a contributes to neuropathic pain by repressing Kcna2 in primary afferent neurons. Nat. Commun 2017; 8: 14712 [PubMed: 28270689]
13. Zhao X, Tang Z, Zhang H, et al. A long noncoding RNA contributes to neuropathic pain by silencing Kcna2 in primary afferent neurons. Nat. Neurosci 2013; 16: 1024–1031 [PubMed: 23792947]
14. Zheng BX, Guo X, Albik S, Eloy J, Tao YX: Effect of Pharmacological Inhibition of Fat-Mass and Obesity-Associated Protein on Nerve Trauma-Induced Pain Hypersensitivities. Neurotherapeutics 2021; 18: 1995–2007 [PubMed: 33829413]
15. Liang L, Lutz BM, Bekker A, Tao YX: Epigenetic regulation of chronic pain. Epigenomics 2015; 7: 235–245 [PubMed: 25942533]
16. Lutz BM, Bekker A, Tao YX: Noncoding RNAs: new players in chronic pain. Anesthesiology 2014; 121: 409–417 [PubMed: 24739997]
17. Liberg D, Sigvardsson M, Akerblad P: The EBF/Olf/Collier family of transcription factors: regulators of differentiation in cells originating from all three embryonal germ layers. Mol. Cell Biol 2002; 22: 8389–8397 [PubMed: 12446759]
18. Lin H, Grosschedl R: Failure of B-cell differentiation in mice lacking the transcription factor EBF. Nature 1995; 376: 263–267 [PubMed: 7542362]
19. Zhang Z, Cotta CV, Stephan RP, deGuzman CG, Klug CA: Enforced expression of EBF in hematopoietic stem cells restricts lymphopoiesis to the B cell lineage. EMBO J 2003; 22: 4759–4769 [PubMed: 12970188]
20. Jimenez MA, Akerblad P, Sigvardsson M, Rosen ED: Critical role for Ebf1 and Ebf2 in the adipogenic transcriptional cascade. Mol. Cell Biol 2007; 27: 743–757 [PubMed: 17060461]
21. Garel S, Marin F, Grosschedl R, Charnay P: Ebf1 controls early cell differentiation in the embryonic striatum. Development 1999; 126: 5285–5294 [PubMed: 10556054]
22. Wang SS, Tsai RY, Reed RR: The characterization of the Olf-1/EBF-like HLH transcription factor family: implications in olfactory gene regulation and neuronal development. J Neurosci 1997; 17: 4149–4158 [PubMed: 9151732]
23. Griffin MJ, Zhou Y, Kang S, Zhang X, Mikkelsen TS, Rosen ED: Early B-cell factor-1 (EBF1) is a key regulator of metabolic and inflammatory signaling pathways in mature adipocytes. J Biol. Chem 2013; 288: 35925–35939 [PubMed: 24174531]

24. Liang L, Zhao JY, Kathryn T, Bekker A, Tao YX: BIX01294, a G9a inhibitor, alleviates nerve injury-induced pain hypersensitivities during both development and maintenance periods. Transl. Perioper. Pain Med 2019; 6: 106–114 [PubMed: 31497620]
25. Yuan J, Wen J, Wu S, et al. Contribution of dorsal root ganglion octamer transcription factor 1 to neuropathic pain after peripheral nerve injury. Pain 2019; 160: 375–384 [PubMed: 30247265]
26. Zhang L, Li X, Feng X, et al. E74-like factor 1 contributes to nerve trauma-induced nociceptive hypersensitivity via transcriptionally activating matrix metalloprotein-9 in dorsal root ganglion neurons. Pain 2022
27. He L, Han G, Wu S, et al. Toll-like receptor 7 contributes to neuropathic pain by activating NF-kappaB in primary sensory neurons. Brain Behav. Immun 2020; 87: 840–851 [PubMed: 32205121]
28. Wen J, Yang Y, Wu S, et al. Long noncoding RNA H19 in the injured dorsal root ganglion contributes to peripheral nerve injury-induced pain hypersensitivity. Transl. Perioper. Pain Med 2020; 7: 176–184 [PubMed: 32099850]
29. Zhang Z, Zheng B, Du S, et al. Eukaryotic initiation factor 4 gamma 2 contributes to neuropathic pain through downregulation of Kv1.2 and the mu opioid receptor in mouse primary sensory neurones. Br. J. Anaesth 2021; 126: 706–719 [PubMed: 33303185]
30. Xu B, Cao J, Zhang J, et al. Role of MicroRNA-143 in Nerve Injury-Induced Upregulation of Dnmt3a Expression in Primary Sensory Neurons. Front Mol. Neurosci 2017; 10: 350 [PubMed: 29170626]
31. Yang Y, Wen J, Zheng B, et al. CREB Participates in Paclitaxel-Induced Neuropathic Pain Genesis Through Transcriptional Activation of Dnmt3a in Primary Sensory Neurons. Neurotherapeutics 2021; 18: 586–600 [PubMed: 33051852]
32. Wang B, Ma L, Guo X, et al. A sensory neuron-specific long noncoding RNA reduces neuropathic pain by rescuing KCNN1 expression. Brain 2023 Apr 4;awad110.doi: 10.1093/brain/awad110
33. Campbell JN, Meyer RA: Mechanisms of neuropathic pain. Neuron 2006; 52: 77–92 [PubMed: 17015228]
34. Fan L, Guan X, Wang W, et al. Impaired neuropathic pain and preserved acute pain in rats overexpressing voltage-gated potassium channel subunit Kv1.2 in primary afferent neurons. Mol. Pain 2014; 10: 8 [PubMed: 24472174]
35. Wu Q, Wei G, Ji F, et al. TET1 Overexpression Mitigates Neuropathic Pain Through Rescuing the Expression of mu-Opioid Receptor and Kv1.2 in the Primary Sensory Neurons. Neurotherapeutics 2019; 16: 491–504 [PubMed: 30515739]
36. Li Z, Mao Y, Liang L, et al. The transcription factor C/EBPbeta in the dorsal root ganglion contributes to peripheral nerve trauma-induced nociceptive hypersensitivity. Sci. Signal 2017; 10: eaam5345 [PubMed: 28698219]
37. Li Z, Gu X, Sun L, et al. Dorsal root ganglion myeloid zinc finger protein 1 contributes to neuropathic pain after peripheral nerve trauma. Pain 2015; 156: 711–721 [PubMed: 25630025]
38. Chien LY, Cheng JK, Chu D, Cheng CF, Tsaur ML: Reduced expression of A-type potassium channels in primary sensory neurons induces mechanical hypersensitivity. J. Neurosci 2007; 27: 9855–9865 [PubMed: 17855600]
39. Ishikawa K, Tanaka M, Black JA, Waxman SG: Changes in expression of voltage-gated potassium channels in dorsal root ganglion neurons following axotomy. Muscle Nerve 1999; 22: 502–507 [PubMed: 10204786]
40. Kim DS, Choi JO, Rim HD, Cho HJ: Downregulation of voltage-gated potassium channel alpha gene expression in dorsal root ganglia following chronic constriction injury of the rat sciatic nerve. Brain Res. Mol. Brain Res 2002; 105: 146–152 [PubMed: 12399117]
41. Rasband MN, Park EW, Vanderah TW, Lai J, Porreca F, Trimmer JS: Distinct potassium channels on pain-sensing neurons. Proc. Natl. Acad. Sci. U. S. A 2001; 98: 13373–13378 [PubMed: 11698689]
42. Yang EK, Takimoto K, Hayashi Y, de Groat WC, Yoshimura N: Altered expression of potassium channel subunit mRNA and alpha-dendrotoxin sensitivity of potassium currents in rat dorsal root ganglion neurons after axotomy. Neuroscience 2004; 123: 867–874 [PubMed: 14751280]

43. Xu Y, Gu Y, Wu P, Li GW, Huang LY: Efficiencies of transgene expression in nociceptive neurons through different routes of delivery of adeno-associated viral vectors. Hum. Gene Ther 2003; 14: 897–906 [PubMed: 12828860]

44. Xu Y, Gu Y, Xu GY, Wu P, Li GW, Huang LY: Adeno-associated viral transfer of opioid receptor gene to primary sensory neurons: a strategy to increase opioid antinociception. Proc. Natl. Acad. Sci. U. S. A 2003; 100: 6204–6209 [PubMed: 12719538]

45. Xu ZZ, Kim YH, et al. Inhibition of mechanical allodynia in neuropathic pain by TLR5-mediated A-fiber blockade. Nat. Med 2015; 21: 1326–1331 [PubMed: 26479925]

Brief Commentary

Background

Neuropathic pain is a complex and debilitating major health problem. Most neuropathic pain patients are non-responsive to the current medications. Thus, identifying new targets and mechanisms for this disorder is clearly an urgent need.

Translational Significance

We demonstrated the downregulation of the early B cell factor 1 (EBF1) in the neurons of injured dorsal root ganglion after peripheral nerve injury. Rescuing this downregulation significantly alleviated the development and maintenance of neuropathic pain. This effect is mediated by reversing nerve injury-induced reduction of Kv1.2 in injured dorsal root ganglion. Findings of this study elucidate the role of EBF1 in neuropathic pain and thereby provide a new avenue for this disorder management.

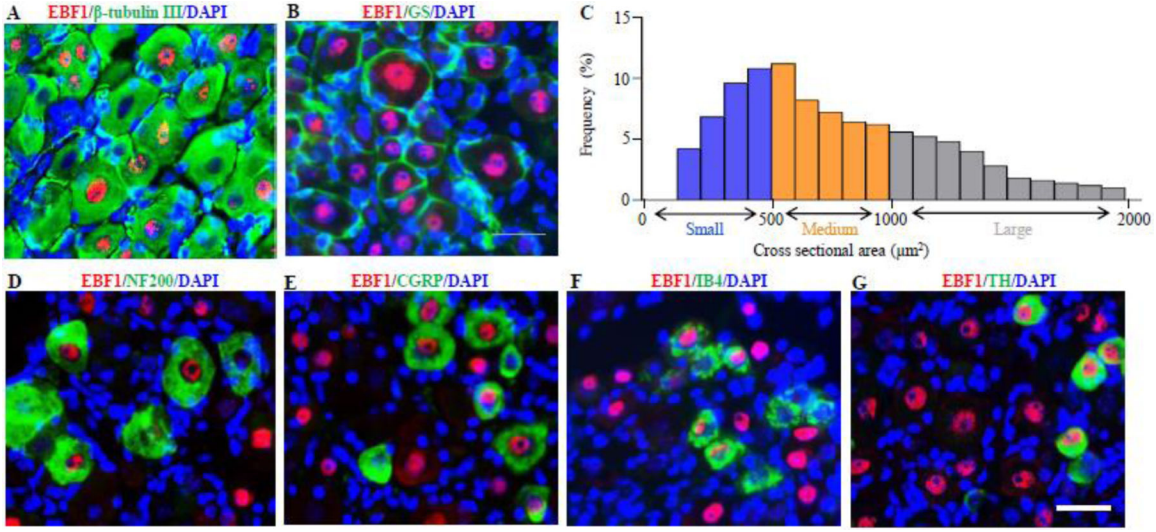

Fig. 1.

Distribution of EBF1 in lumbar dorsal root ganglion of naïve mice. (A, B) Double-label immunofluorescent staining showed co-expression of nuclear EBF1 (red) with cytoplasmic β-tubulin III (green; A), but not with cytoplasmic glutamine synthetase (GS; green; B), in individual DRG cells. Cellular nuclei were labeled by 4',6-diamidino-2-phenylindole (DAPI; blue). n = 3 mice. Scale bar: 30 μm. (C) Size distribution of EBF1-positive neuronal somata in naïve DRG. Large, 29.4%; medium: 39.2%; small: 31.4%. (D-G) Double-labeled immunofluorescent staining showed co-expression of nuclear EBF1 (red) with cytoplasmic neurofilament 200 (NF200; green; D), calcitonin gene-related peptide (CGPR; green; E), isolectin B4 (IB4; green; F), or tyrosine hydroxylase (TH; green; G) in individual DRG neurons. Cellular nuclei were labeled by DAPI (blue). n = 3 mice. Scale bar: 30 μm.

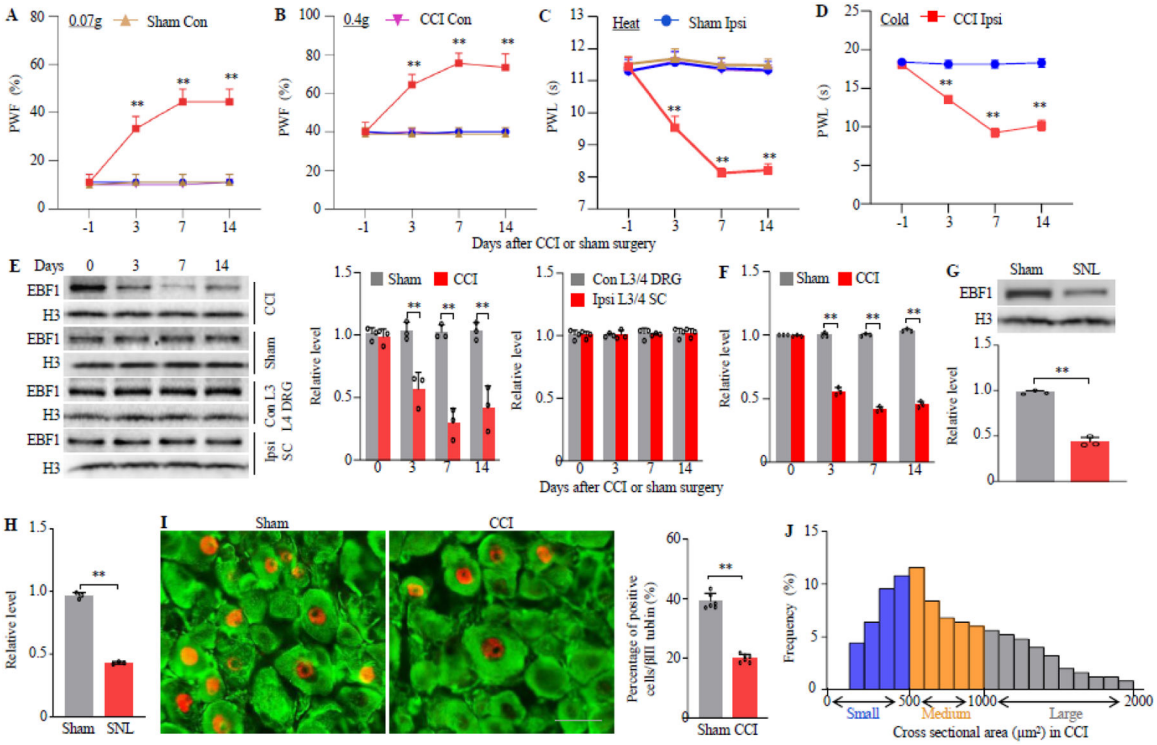

Fig. 2.

Peripheral nerve injury-induced downregulation of EBF1 expression in injured dorsal root ganglion. (A-D) Paw withdrawal frequencies (PWF) in response to 0.07 g (A) and 0.4 g (B) von Frey filament stimuli and paw withdrawal latencies (PWL) to heat (C) and cold (D) stimuli on the ipsilateral (Ipsi) and contralateral (Con) on days −1, 3, 7, and 14 after CCI or sham surgery. n = 9 mice/group. $^{**}P<0.01$ *vs* sham group on the ipsilateral side at the corresponding time points by two-way ANOVA with repeated measures followed by post hoc Tukey test. (E, F) Expression of EBF1 protein (E) and *Ebf1* mRNA (F) in the ipsilateral (Ipsi) L3/4 DRGs, contralateral (Con) L3/4 DRGs and ipsilateral L3/4 spinal cord (SC) on days 0, 3, 7 and 14 after CCI or sham surgery. n = 3 repeats (6 mice)/time point. $^{**}P<0.01$ by two-way ANOVA followed by post hoc Tukey test. (G, H) Expression of EBF1 protein (G) and *Ebf1* mRNA (H) in the ipsilateral L4 DRG on day 7 after SNL or sham surgery. n = 3 repeats (6 mice)/time point. $^{**}P<0.01$ by the two-tailed unpaired Student *t* test. (I) Representative immunofluorescent images (left) and statistical summary (right) of the number of EBF1 (red)-positive neurons (marked by β-tubulin III; green) in the ipsilateral L4 DRG on day 7 after CCI or sham surgery. n = 6 mice. $^{**}P<0.01$ by two-tailed unpaired Student *t* test. Scale bar: 30 μm. (J) Size distribution of EBF1-positive neuronal somata in the ipsilateral L4 DRG on day 7 after CCI. Large, 29.6%; medium: 39.2%; small: 31.2%.

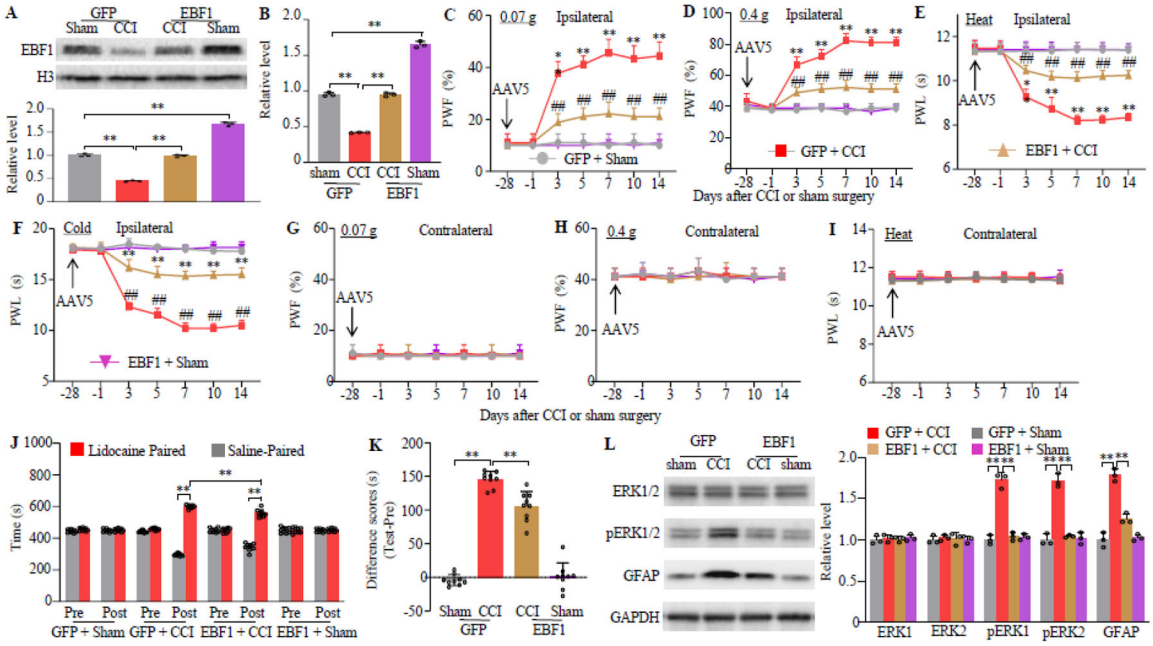

Fig. 3.

Effect of DRG microinjection of AAV5-*Ebf1* on the development of CCI-induced nociceptive hypersensitivity in male mice. (A, B) Expression of EBF1 protein (A) and *Ebf1* mRNA (B) in the ipsilateral L3/4 DRGs on day 14 after CCI or sham surgery in mice with microinjection with AAV5-*Ebf1* (EBF1) or AAV5-*Gfp* (GFP) into unilateral L3/4 DRGs 28 days before surgery. n = 3 repeats (6 mice)/group. $^{**}P < 0.01$ by two-way ANOVA followed by post hoc Tukey test. (C-I) Paw withdrawal frequencies (PWF) in response to 0.07 g (C, G) and 0.4 g (D, H) von Frey filament stimuli and paw withdrawal latencies (PWL) to heat (E, I) and cold (F) stimuli on the ipsilateral (C-F) and contralateral (G-I) sides at the different days as indicated after CCI or sham surgery in mice with microinjection of AAV5-*Ebf1* (EBF1) or AAV5-*Gfp* (GFP) into unilateral L3/4 DRGs 28 days before surgery. n = 9 mice/group. $^{**}P < 0.01$ *vs* the AAV5-*Gfp*-microinjected sham group at the corresponding days and $^{\#\#}P < 0.01$ *vs* the AAV5-*Gfp*-microinjected CCI group at the corresponding days by three-way ANOVA with repeated measures followed by post hoc Tukey test. (J, K) Effect of microinjection of AAV5-*Ebf1* (EBF1) or AAV5-*Gfp* (GFP) into unilateral L3/4 DRGs on spontaneous nociceptive responses as assessed by the CPP paradigm on day 14 post-surgery. Time spent in each chamber (J) and difference scores for chamber preferences calculated by subtracting preconditioning (Pre) preference time from postconditioning (Post) time spent in the lidocaine-paired chamber (K). n = 9 mice/group. $^{**}P < 0.01$ by three-way ANOVA with repeated measures followed by post hoc Tukey test (J) or by two-way ANOVA with repeated measures followed by post hoc Tukey test (K). (L) Expression of p-ERK1/2, total ERK1/2, and GFAP in the ipsilateral L3/4 dorsal horn on day 14 after CCI or sham surgery in mice with microinjection of AAV5-*Ebf1* (EBF1) or AAV5-*Gfp* (GFP) into unilateral L3/4 DRGs 28 days before surgery. n = 3 repeats (6 mice)/group. $^{**}P < 0.01$ by two-way ANOVA followed by post hoc Tukey test.

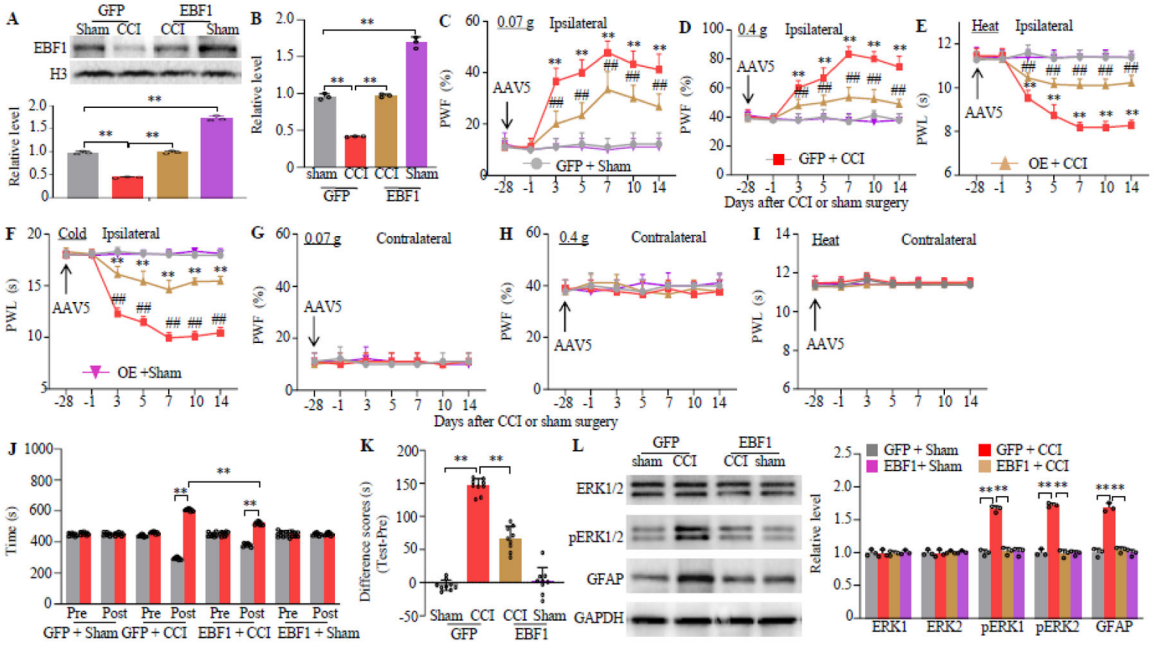

Fig. 4.

Effect of DRG microinjection of AAV5-*Ebf1* on the development of CCI-induced nociceptive hypersensitivity in female mice. (A, B) Expression of EBF1 protein (A) and *Ebf1* mRNA (B) in the ipsilateral L3/4 DRGs on day 14 after CCI or sham surgery in mice with microinjection with AAV5-*Ebf1* (EBF1) or AAV5-*Gfp* (GFP) into unilateral L3/4 DRGs 28 days before surgery. n = 3 repeats (6 mice)/group. $^{**}P < 0.01$ by two-way ANOVA followed by post hoc Tukey test. (C-I) Paw withdrawal frequencies (PWF) in response to 0.07 g (C, G) and 0.4 g (D, H) von Frey filament stimuli and paw withdrawal latencies (PWL) to heat (E, I) and cold (F) stimuli on the ipsilateral (C-F) and contralateral (G-I) sides at the different days as indicated after CCI or sham surgery in mice with microinjection of AAV5-*Ebf1* (EBF1) or AAV5-*Gfp* (GFP) into unilateral L3/4 DRGs 28 days before surgery. n = 9 mice/group. $^{**}P < 0.01$ *vs* the AAV5-*Gfp*-microinjected sham group at the corresponding days and $^{\#\#}P < 0.01$ *vs* the AAV5-*Gfp*-microinjected CCI group at the corresponding days by three-way ANOVA with repeated measures followed by post hoc Tukey test. (J, K) Effect of microinjection of AAV5-*Ebf1* (EBF1) or AAV5-*Gfp* (GFP) into unilateral L3/4 DRGs on spontaneous nociceptive responses as assessed by the CPP paradigm on day 14 post-surgery. Time spent in each chamber (J) and difference scores for chamber preferences calculated by subtracting preconditioning (Pre) preference time from postconditioning (Post) time spent in the lidocaine-paired chamber (K). n = 9 mice/group. $^{**}P < 0.01$ by three-way ANOVA with repeated measures followed by post hoc Tukey test (J) or by two-way ANOVA with repeated measures followed by post hoc Tukey test (K). (L) Expression of p-ERK1/2, total ERK1/2, and GFAP in the ipsilateral L3/4 dorsal horn on day 14 after CCI or sham surgery in mice with microinjection of AAV5-*Ebf1* (EBF1) or AAV5-*Gfp* (GFP) into unilateral L3/4 DRGs 28 days before surgery. n = 3 repeats (6 mice)/group. $^{**}P < 0.01$ by two-way ANOVA followed by post hoc Tukey test.

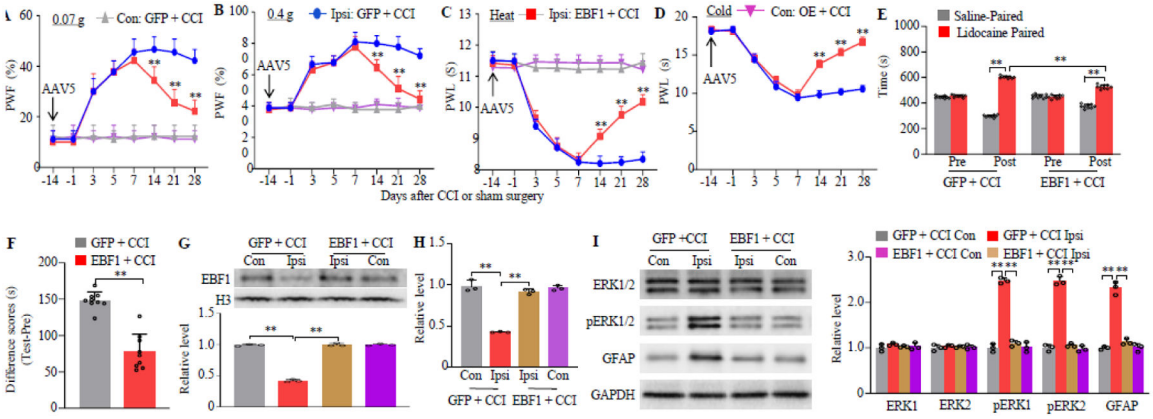

Fig. 5.

Effect of DRG microinjection of AAV5-*Ebf1* on the maintenance of CCI-induced nociceptive hypersensitivity in male mice. (A-D) Paw withdrawal frequencies (PWF) in response to 0.07 g (A) and 0.4 g (B) von Frey filament stimuli and paw withdrawal latencies (PWL) to heat (C) and cold (D) stimuli on the ipsilateral (Ipsi) and contralateral (Con) sides at the different days as indicated after CCI in mice with microinjection of AAV5-*Ebf1* (EBF1) or AAV5-*Gfp* (GFP) into unilateral L3/4 DRGs 14 days before surgery. n = 9 mice/group. $^{**}P < 0.01$ *vs* the AAV5-*Gfp*-microinjected CCI group at the corresponding days by three-way ANOVA with repeated measures followed by post hoc Tukey test. (E, F) Effect of microinjection of AAV5-*Ebf1* (EBF1) or AAV5-*Gfp* (GFP) into unilateral L3/4 DRGs on spontaneous nociceptive responses as assessed by the CPP paradigm on day 28 post-surgery. Time spent in each chamber (E) and difference scores for chamber preferences calculated by subtracting preconditioning (Pre) preference time from postconditioning (Post) time spent in the lidocaine-paired chamber (F). n = 9 mice/group. $^{**}P < 0.01$ by three-way ANOVA with repeated measures followed by post hoc Tukey test (E) or by two-tailed unpaired Student *t* test (F). (G, H) Expression of EBF1 protein (G) and *Ebf1* mRNA (H) in the ipsilateral (Ipsi) and contralateral (Con) L3/4 DRGs on day 28 after CCI in mice with microinjection of AAV5-*Ebf1* (EBF1) or AAV5-*Gfp* (GFP) into unilateral L3/4 DRGs 14 days before surgery. n = 3 repeats (6 mice)/group. $^{**}P < 0.01$ by two-way ANOVA followed by post hoc Tukey test. (I) Expression of p-ERK1/2, total ERK1/2, and GFAP in the ipsilateral (Ipsi) and contralateral (Con) L3/4 dorsal horn on day 28 after CCI in mice with microinjection of AAV5-*Ebf1* (EBF1) or AAV5-*Gfp* (GFP) into unilateral L3/4 DRGs 14 days before surgery. n = 3 repeats (6 mice)/group. $^{**}P < 0.01$ by two-way ANOVA followed by post hoc Tukey test.

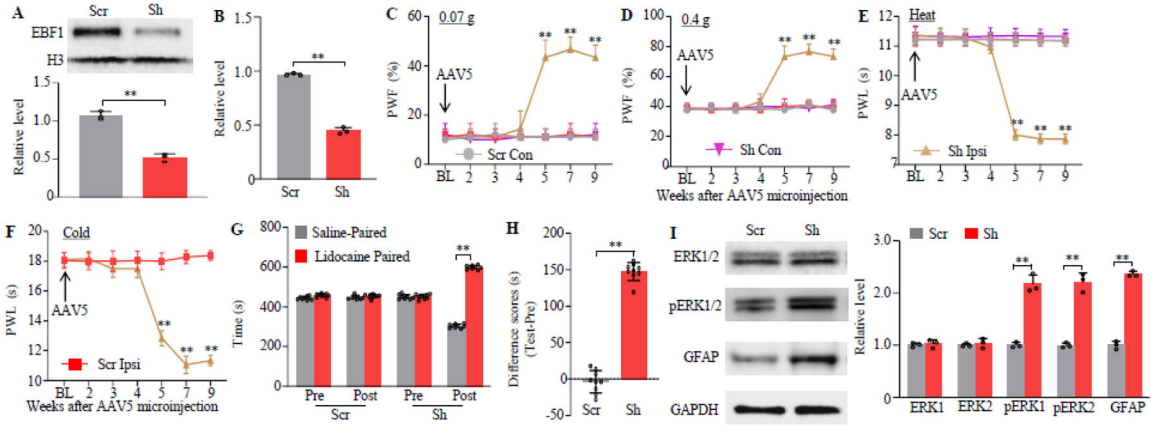

Fig. 6.

Effects of DRG EBF1 knockdown on basal nociceptive thresholds in male mice. (A, B) Expression of EBF1 protein (A) and *Ebf1* mRNA (B) in the ipsilateral L3/4 DRGs on week 9 after microinjection of AAV5-*Ebf1* shRNA (Sh) or AAV5-*scrambled* shRNA (Scr) into unilateral L3/4 DRGs. n = 3 repeats (6 mice)/group. $^{**}P < 0.01$ by two-tailed unpaired Student *t* test. (C-F) Paw withdrawal frequencies (PWF) in response to 0.07 g (C) and 0.4 g (D) von Frey filament stimuli and paw withdrawal latencies (PWL) to heat (E) and cold (F) stimuli on the ipsilateral (Ipsi) and contralateral (Con) sides at the different weeks as indicated after microinjection of AAV5-*Ebf1* shRNA (Sh) or AAV5-*scrambled* shRNA (Scr) into unilateral L3/4 DRGs. n = 9 mice/group. $^{**}P < 0.01$ *vs* the AAV5-*scrambled* shRNA-microinjected group at the corresponding days by three-way ANOVA with repeated measures followed by post hoc Tukey test. (G, H) Effect of microinjection of AAV5-*Ebf1* shRNA (Sh) or AAV5-*scrambled* shRNA (Scr) into unilateral L3/4 DRGs on spontaneous nociceptive responses as assessed by the CPP paradigm on week 8 post-microinjection. Time spent in each chamber (G) and difference scores for chamber preferences calculated by subtracting preconditioning (Pre) preference time from postconditioning (Post) time spent in the lidocaine-paired chamber (H). n = 9 mice/group. $^{**}P < 0.01$ by three-way ANOVA with repeated measures followed by post hoc Tukey test (G) or by two-tailed unpaired Student *t* test (H). (I) Expression of p-ERK1/2, total ERK1/2, and GFAP in the ipsilateral L3/4 dorsal horn on week 9 after microinjection of AAV5-*Ebf1* shRNA (Sh) or AAV5-*scrambled* shRNA (Scr) into unilateral L3/4 DRGs. n = 3 repeats (6 mice)/group. $^{**}P < 0.01$ by two-tailed unpaired Student *t* test.

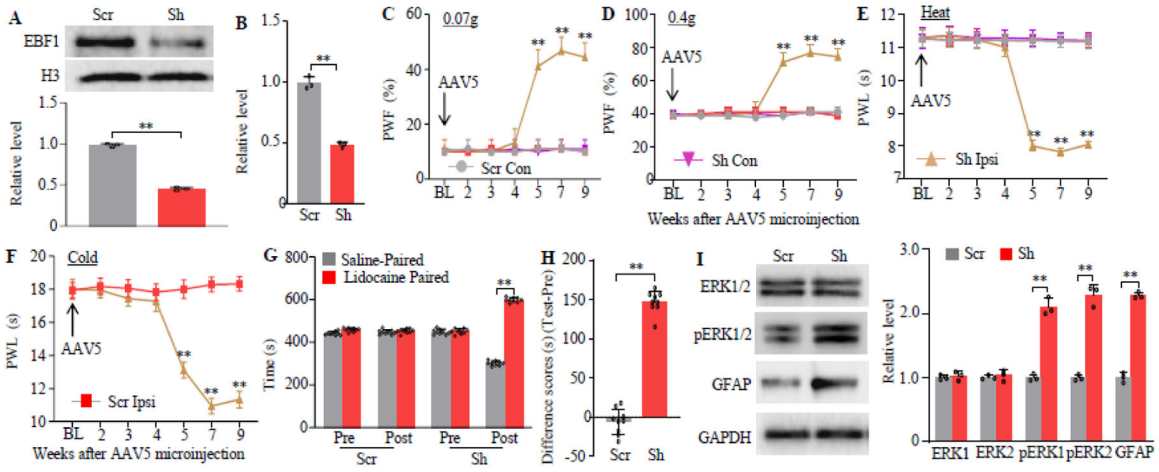

Fig. 7.

Effects of DRG EBF1 knockdown on basal nociceptive thresholds in female mice. (A, B) Expression of EBF1 protein (A) and *Ebf1* mRNA (B) in the ipsilateral L3/4 DRGs on week 9 after microinjection of AAV5-*Ebf1* shRNA (Sh) or AAV5-*scrambled* shRNA (Scr) into unilateral L3/4 DRGs. n = 3 repeats (6 mice)/group. $^{**}P < 0.01$ by two-tailed unpaired Student *t* test. (C-F) Paw withdrawal frequencies (PWF) in response to 0.07 g (C) and 0.4 g (D) von Frey filament stimuli and paw withdrawal latencies (PWL) to heat (E) and cold (F) stimuli on the ipsilateral (Ipsi) and contralateral (Con) sides at the different weeks as indicated after microinjection of AAV5-*Ebf1* shRNA (Sh) or AAV5-*scrambled* shRNA (Scr) into unilateral L3/4 DRGs. n = 9 mice/group. $^{**}P < 0.01$ *vs* the AAV5-*scramled* shRNA-microinjected group at the corresponding days by three-way ANOVA with repeated measures followed by post hoc Tukey test. (G, H) Effect of microinjection of AAV5-*Ebf1* shRNA (Sh) or AAV5-*scrambled* shRNA (Scr) into unilateral L3/4 DRGs on spontaneous nociceptive responses as assessed by the CPP paradigm on week 8 post-microinjection. Time spent in each chamber (G) and difference scores for chamber preferences calculated by subtracting preconditioning (Pre) preference time from postconditioning (Post) time spent in the lidocaine-paired chamber (H). n = 9 mice/group. $^{**}P < 0.01$ by three-way ANOVA with repeated measures followed by post hoc Tukey test (G) or by two-tailed unpaired Student *t* test (H). (I) Expression of p-ERK1/2, total ERK1/2, and GFAP in the ipsilateral L3/4 dorsal horn on week 9 after microinjection of AAV5-*Ebf1* shRNA (Sh) or AAV5-*scrambled* shRNA (Scr) into unilateral L3/4 DRGs. n = 3 repeats (6 mice)/group. $^{**}P < 0.01$ by two-tailed unpaired Student *t* test.

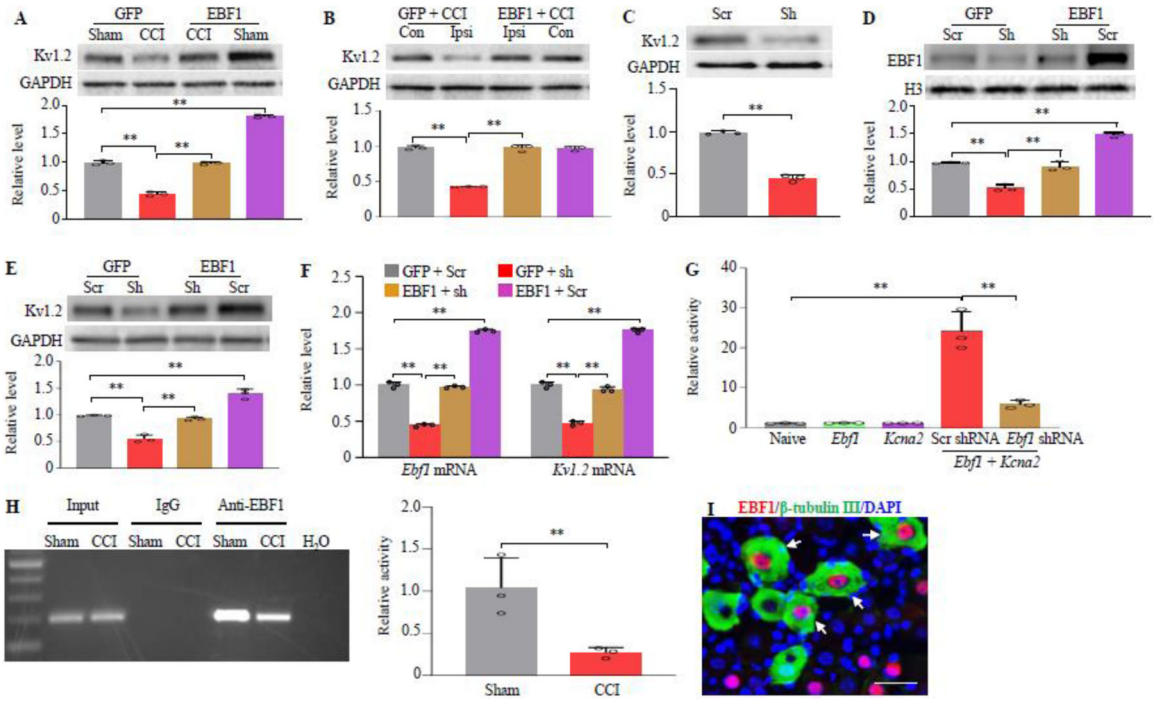

Fig. 8.

Role of downregulated DRG EBF1 in CCI-induced decrease of Kv1.2 in injured DRG. (A) Expression of Kv1.2 in the ipsilateral L3/4 DRGs on day 14 after CCI or sham surgery in male mice with microinjection of AAV5-*Ebf1* or AAV5-*Gfp* into unilateral L3/4 DRGs 28 days before surgery. n = 3 repeats (6 mice)/group. $^{**}P < 0.01$ by two-way ANOVA followed by post hoc Tukey test. (B) Expression of Kv1.2 in the ipsilateral (Ipsi) and contralateral (Con) L3/4 DRGs on day 28 after CCI in mice with microinjection of AAV5-*Ebf1* (EBF1) or AAV5-*Gfp* (GFP) into unilateral L3/4 DRGs 14 days before surgery. n = 3 repeats (6 mice)/group. $^{**}P < 0.01$ by two-way ANOVA followed by post hoc Tukey test. (C) Expression of Kv1.2 in the ipsilateral L3/4 DRGs on week 9 after microinjection of AAV5-*Ebf1* shRNA (Sh) or AAV5-*scrambled* shRNA (Scr) into unilateral L3/4 DRGs. n = 3 repeats (6 mice)/group. $^{**}P < 0.01$ by two-tailed unpaired Student *t* test. (D-F) Expression of EBF1 protein (D), Kv1.2 protein (E) and their mRNAs (F) in the cultured DRG neurons with co-transduction of viruses as indicated. GFP: AAV5-*Gfp*. EBF1: AAV5-*Ebf1*. Sh: AAV5-*Ebf1* shRNA. Scr: AAV5-*scrambled* shRNA. n = 3 repeats/group. $^{**}P < 0.01$ by one-way ANOVA followed by post hoc Tukey test. (G) *Kcan2* gene promoter activity in the CAD cells transfected with the vectors and transduced with the virus as shown. Naive: empty pGL3-Basic. *Kcan2*: pGL3-*Kcna2* report vector. *Ebf1* shRNA: AAV5-*Ebf1* shRNA. Scr shRNA: AAV5-*scrambled* shRNA. EBF1: AAV5-*Ebf1*. n = 3 repeats/group. $^{**}P < 0.01$ by one-way ANOVA followed by Tukey post hoc test. (H) *Kvcna2* gene promoter fragment immunoprecipitated by anti-EBF1 antibody in the ipsilateral L3/4 DRGs on day 7 post-CCI or sham surgery. Input: total purified fragments. n = 3 repeats (15 mice)/group. $^{**}P < 0.01$ by two-tailed unpaired Student *t* test. (I) Co-expression of nuclear EBF1 (red) with cytoplasmic/membrane Kv1.2 (green) in individual DRG neurons (arrows) from naïve mice. Cellular nuclei were labeled by 4',6-diamidino-2-phenylindole (DAPI; blue). n = 3 mice. Scale bar: 30 μm.

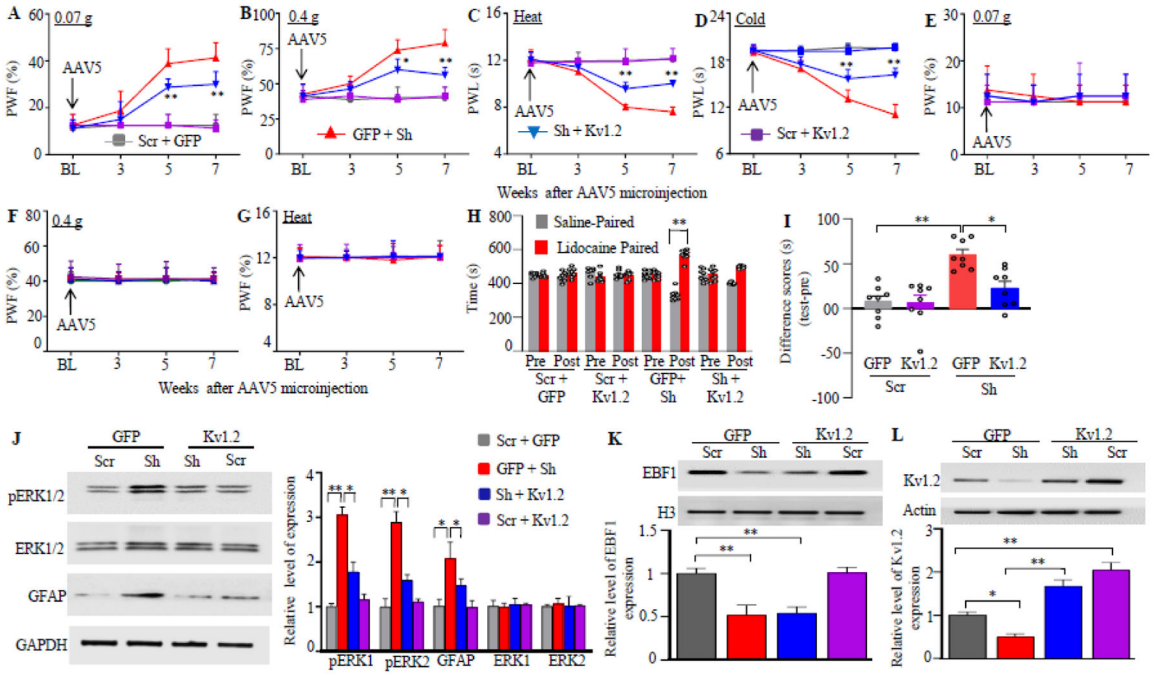

Fig. 9.

Effect of rescuing DRG Kv1.2 expression on DRG EBF1 knockdown-induced nociceptive hypertsensitivity in naïve male mice. (A-G) Paw withdrawal frequencies (PWF) in response to 0.07 g (A, E) and 0.4 g (B, F) von Frey filament stimuli and paw withdrawal latencies (PWL) to heat (C, G) and cold (D) stimuli on the ipsilateral (A-D) and contralateral (E-G) sides at the different weeks as indicated after microinjection of AAV5-GFP (GFP) plus AAV5-*scrambled* shRNA (Scr), GFP plus AAV5-*Ebf1* shRNA (Sh), AAV5-Kv1.2 (Kv1.2) plus Sh, or Kv1.2 plus Scr into unilateral L3/4 DRGs. n = 8 mice/group. $*P < 0.05$ or $**P < 0.01$ *vs* the GFP plus Sh group at the corresponding time points by two-way ANOVA with repeated measures followed by Tukey post hoc test. (H, I) Time spent in each chamber (H) and difference scores for chamber preferences calculated by subtracting preconditioning (Pre) preference time from postconditioning (Post) time spent in the lidocaine-paired chamber (I). n = 8 mice/group. $**P < 0.01$ by three-way ANOVA with repeated measures followed by post hoc Tukey test (H) or by two-tailed unpaired Student *t*-test (I). (J) Expression of p-ERK1/2, total ERK1/2, and GFAP in the ipsilateral L3/4 dorsal horn on week 7 after microinjection of AAV5-GFP (GFP) plus AAV5-*scrambled* shRNA (Scr), GFP plus AAV5-*Ebf1* shRNA (Sh), AAV5-Kv1.2 (Kv1.2) plus Sh, or Kv1.2 plus Scr into unilateral L3/4 DRGs. n = 3 repeats (6 mice)/group. $**P < 0.01$ by ne-way ANOVA followed by post hoc Tukey test. (K, L) Expression of EBF1 (K) and Kv1.2 (L) in the ipsilateral L3/4 DRGs 7 weeks after microinjection of AAV5-GFP (GFP) plus AAV5-*scrambled* shRNA (Scr), GFP plus AAV5-*Ebf1* shRNA (Sh), AAV5-Kv1.2 (Kv1.2) plus Sh, or Kv1.2 plus Scr into unilateral L3/4 DRGs. n = 3 repeats (6 mice)/group. $**P < 0.01$ by one-way ANOVA followed by post hoc Tukey test.